Radiology

^{18}F-16α-17β-Fluoroestradiol Binding Specificity in Estrogen Receptor–Positive Breast Cancer[1]

Kelley Salem, PhD
Manoj Kumar, MS
Ginny L. Powers, PhD[2]
Justin J. Jeffery, BS
Yongjun Yan, PhD
Aparna M. Mahajan, MD
Amy M. Fowler, MD, PhD

Purpose: To determine the binding specificity of ^{18}F-16α-17β-fluoroestradiol (FES) in estrogen receptor (ER) α–positive breast cancer cells and tumor xenografts.

Materials and Methods: Protocols were approved by the office of biologic safety and institutional animal care and use committee. By using ER-negative MDA-MB-231 breast cancer cells, clonal lines were created that expressed either wild-type (WT; 231 WT ER) or G521R mutant ERα (231 G521R ER), which is defective in estradiol binding. ERα protein levels, subcellular localization, and transcriptional function were confirmed. FES binding was measured by using an in vitro cell uptake assay. In vivo FES uptake was measured in tumor xenografts by using small-animal positron emission tomographic/computed tomographic imaging of 24 mice (17 WT ER tumors, nine mutant G521R ER tumors, eight MDA-MB-231 tumors, and four MCF-7 ER-positive tumors). Statistical significance was determined by using Mann-Whitney (Wilcoxon rank sum) test.

Results: ERα transcriptional function was abolished in the mutated 231 G521R ER cells despite appropriate receptor protein expression and nuclear localization. In vitro FES binding in the 231 G521R ER cells was reduced to that observed in the parental cells. Similarly, there was no significant FES uptake in the 231 G521R ER xenografts (percent injected dose [ID] per gram, 0.49 ± 0.042), which was similar to the negative control MDA-MB-231 xenografts (percent ID per gram, 0.42 ± 0.051; P = .20) and nonspecific muscle uptake (percent ID per gram, 0.41 ± 0.0095; P = .06).

Conclusion: This study showed that FES retention in ER-positive breast cancer is strictly dependent on an intact receptor ligand-binding pocket and that FES binds to ERα with high specificity. These results support the utility of FES imaging for assessing tumor heterogeneity by localizing immunohistochemically ER-positive metastases that lack receptor-binding functionality.

©RSNA, 2017

Online supplemental material is available for this article.

Radiology

Breast cancers routinely undergo testing for biomarkers, including estrogen receptor (ER) α, progesterone receptor, and human epidermal growth factor receptor type 2, that provide prognostic and predictive information to guide treatment decisions. Endocrine-based therapies are aimed at directly antagonizing ERα function, depleting endogenous estrogen, or degrading ERα protein to stop estrogen-stimulated tumor growth. Unfortunately, resistance to endocrine therapy is frequent and has resulted in a need for accurate methods to determine endocrine sensitivity and ERα functionality.

Molecular imaging of breast cancer is a promising noninvasive approach to guide treatment decisions and help predict response. Whole-body positron emission tomography (PET) imaging

of ERα with radiolabeled estrogen, ^{18}F-16α-17β-fluoroestradiol (FES), can be used to help to determine the receptor status of all disease sites simultaneously and is particularly helpful when lesions suspected of being metastatic cannot be biopsied. FES PET may also be a useful predictive imaging biomarker for treatment response. Studies (1,2) show that patients who have metastatic breast lesions with maximum standard uptake value below 1.5 are unlikely to benefit from endocrine therapy. This finding is being prospectively studied through a multi-institutional phase II clinical trial in the Unites States. Furthermore, FES PET imaging is increasingly being used in European clinical practice (3,4).

Critical to implementation of FES PET imaging into clinical care is its ability to accurately depict ERα protein expression. FES binds the ERα receptor subtype with high binding affinity and selectivity (5,6). FES maximum standard uptake value correlates well with ERα protein expression (7–10). Overall sensitivity of FES PET for detection of ER-positive breast cancer was 82% (95% confidence interval: 74%, 88%) and overall specificity in lesions shown to be benign with histologic analysis and ER-negative breast cancer was high at 95% (95% confidence interval: 86%, 99%) (7,8,11–14).

High-fidelity binding of FES is important to prevent false-positive

interpretation. Binding specificity has been inferred indirectly by demonstrating reduced FES uptake when co-administered with unlabeled estradiol (5,15–18). This is also evidenced in animal models and patients who are administered ERα antagonists that compete with FES for the ligand-binding domain (19–22). Nonspecific FES binding may overestimate ERα expression and falsely indicate a high likelihood of response to endocrine therapy or insufficient antagonist drug dosing. In our study, we used a direct approach for testing FES binding specificity by which ERα is genetically altered to determine whether any sites for FES binding exist beyond the receptor ligand binding pocket. We hypothesized that breast cancer cells and tumors that express mutant ER protein that is incapable of binding estradiol would show no significant uptake of FES. The purpose of this study was to determine the binding specificity of FES in ERα-positive breast cancer cells and tumor xenografts.

Materials and Methods

The overall experimental design is illustrated in Figure 1. To test the specificity of FES for the ligand-binding domain of ERα, we first generated stable cell lines constitutively expressing

Advances in Knowledge

- Stable, constitutive expression of wild-type (WT) estrogen receptor (ER) α in MDA-MB-231 cells behaved similarly to endogenously expressed ERα; however, the G521R ligand-binding domain mutation rendered the receptor functionally null despite appropriate protein expression and nuclear localization.

- Whereas ^{18}F-16α-17β-fluoroestradiol (FES) competitive binding curves appeared similar in the 231 WT ER cells to the ER-positive MCF-7 cells, there was no specific FES binding in the 231 G521R ER cells, which behaved similarly to the parental MDA-MB-231 cells.

- Tumor-to-muscle ratios of FES uptake by using PET/CT imaging were 0.97 ± 0.07 in MDA-MB-231 xenografts, 2.1 ± 0.10 in 231 WT ER xenografts, and 1.1 ± 0.08 in 231 G521R ER xenografts, which demonstrated a lack of FES retention ($P = .20$ compared with parental MDA-MB-231 xenografts) despite robust protein expression of G521R ERα in tumor xenografts.

Implications for Patient Care

- ERα positivity by immunohistochemistry indicates the presence, but not functionality, of ERα protein, which may be better assessed by using FES PET imaging.

- These results support the utility of FES PET imaging for assessing intrapatient, intermetastatic tumor heterogeneity by localizing immunohistochemically ER-positive lesions that lack receptor-binding functionality, which could direct further tissue biopsy for genomic analysis and optimize treatment.

Figure 1

Figure 1: Overall experimental design. Stable cell lines were generated and characterized by using in vitro assays measuring ERα protein expression, nuclear localization, and transcriptional function. Tumor xenografts were grown in 24 female athymic nude mice and imaged by using FES PET/computed tomography (CT). Nine mice had one tumor xenograft each (right thoracic mammary fat pad) and 15 mice had two tumor xenografts each (one in the right thoracic mammary fat pad, one in the left thoracic mammary fat pad). After imaging, tumors were excised and analyzed for ERα protein expression by immunohistochemistry and Western blot analysis. WT = wild type.

either wild type ERα or G521R mutated ERα. The mutation of glycine521 to arginine in the human *ESR1* gene is equivalent to the G525R mutation in the mouse *ESR1* gene, which causes loss of estradiol binding (23). To our knowledge, this mutation has not yet been found in human breast cancers but represents a useful tool for modeling a receptor deficient in ligand-binding function. The generated stable cell lines were then characterized by using in vitro assays that measured ERα protein expression, nuclear localization, and transcriptional function. Tumor xenografts were grown in female athymic nude mice and imaged by using FES PET/CT. After imaging, tumors were excised and analyzed for ERα protein expression by immunohistochemistry and Western blot analysis. Because of the inability of the G521R mutant ERα to bind estradiol, we hypothesized that FES uptake would be completely abolished if the binding of FES was strictly dependent on the ligand-binding pocket. If nonspecific binding of FES occurred outside of the ligand-binding pocket, then residual binding and uptake would be measured in the 231 G521R ER cells.

Cell Culture

Experiments were performed by using a protocol approved by the office of biologic safety. ERα-positive (MCF-7) and ERα-negative (MDA-MB-231) human breast cancer cell lines were obtained from the Mallinckrodt Institute of Radiology Pre-Clinical PET/CT Imaging Facility (Washington University School of Medicine, St Louis, Mo). Authentication was performed by using short tandem repeat analysis. Cells were cultured in Dulbecco's modified Eagle's medium (Corning, Corning, NY), supplemented with 10% fetal bovine serum (Corning) and 1% penicillin and streptomycin (Gibco, Waltham, Mass) at 37°C and 10% CO_2. For estrogen-depleted conditions, cells were grown in phenol red-free Dulbecco's modified Eagle's medium with 10% steroid-stripped fetal bovine serum, 2 mmol/L of L-glutamine, and 1% penicillin and streptomycin at 37°C and 5% CO_2.

Stable clonal cell lines that expressed either WT ERα (231 WT ER) or mutant G521R (231 G521R ER) were created by transfecting MDA-MB-231 cells with an expression plasmid containing WT or mutant G521R ERα cDNA (24) by using previously described methods (25). Cells were initially selected by using 1000 μg/mL and maintained with 200 μg/mL hygromycin B (Life Technologies, Waltham, Mass).

In Vitro Assays

The methods used for immunofluorescence, Western blot analysis, reporter gene assays, and quantitative real-time polymerase chain reaction are included in Appendix E1 (online).

Tumor Xenografts

Experiments were performed according to the American Association for Laboratory Animal Science guidelines with an approved protocol. Twenty-five female athymic NCr-nu/nu mice aged 6 weeks were orthotopically injected with 1.5×10^6 cells at 1:1 ratio with Matrigel (BD Biosciences, San Jose, Calif) into the thoracic mammary fat pad. Palpable tumors formed in 24 of the 25 injected mice. Nine mice had one tumor xenograft each (right thoracic mammary fat pad) and 15 mice had two tumor xenografts each (one in the right thoracic mammary fat pad, one in the left thoracic mammary fat pad). There were eight tumors for the MDA-MB-231 xenografts, 17 tumors for the 231 WT ER xenografts, nine tumors for the 231 mutant G521R ER xenografts, and four tumors for the MCF-7 ER-positive xenografts. Tumor diameters were measured with calipers, and volumes were calculated by using the formula $[a \cdot b^2/2]$, where a is the long diameter and b is the short diameter.

MCF-7 cells were used as a positive control to confirm correct FES radiosynthesis because this ER-positive tumor xenograft model was previously shown to have strong FES uptake (22). Because estrogen supplementation is required for MCF-7 xenograft formation, mice were given 17β-estradiol (E_2; 10 μg/mL) in their drinking water

until 2 days before they underwent FES imaging.

FES Cell Uptake Assay and Small-Animal PET/CT Imaging

FES was synthesized by our radiopharmaceutical production facility after a previously reported method (26) with minor modifications. Specific activity at the end of synthesis exceeded 55.3 GBq/μmol (1495 mCi/μmol).

For cell uptake assays, cells were plated 1.5×10^5 per well in 24-well plates. After overnight incubation, cells were washed twice with phosphate-buffered saline and grown in estrogen-depleted media. The following day, cells were incubated for 1 hour at 37°C with 0.037 MBq (1 μCi) of FES added per well with unlabeled 17β-estradiol (10^{-13} to 10^{-8} mol/L) or ethanol vehicle control. Cells were washed three times with phosphate-buffered saline and lysed with 1 normal NaOH. Collected radioactivity was measured with a γ counter (2480 Wizard²; Perkin Elmer, Waltham, Mass) and corrected for decay. Data for MCF-7 and 231 WT ER cells are shown as percent maximum uptake values (samples containing FES with no cold E_2 added were 100%). Because no specific uptake of FES was observed above background levels (samples without FES) for MDA-MB-231 and 231 G521R ER cells, these values are expressed relative to MCF-7 cells. Half-maximal inhibitory concentration was determined by using nonlinear regression–to–dose response inhibition. Three independent experiments were performed.

Twenty-four mice underwent FES PET/CT imaging. The number of tumors measured with PET imaging was as follows: eight for the MDA-MB-231 xenografts, 17 for the 231 WT ER xenografts, nine for the 231 mutant G521R ER xenografts, and four for the MCF-7 ER-positive xenografts. For imaging, mice with tumor volumes of at least 100 mm³ were injected in the tail vein with 9.25 MBq (250 μCi) FES, anesthetized with 1.5%–2.0% isoflurane, and scanned supine in a dedicated small-animal PET/CT scanner (Inveon; Siemens Preclinical Solutions, Knoxville, Tenn) 1

hour after injection with FES. PET/CT images were co-registered and analyzed (Inveon Research Workplace 3.0; Siemens Medical Solutions, Malvern, Pa). One of the authors (M.K., a research assistant with 3 years of experience with small animal PET/CT imaging) drew the regions of interest with training by the senior author (A.M.F., the principal investigator with 7 years of experience). Regions of interest were drawn around the tumor and within quadriceps and triceps muscles. The average volume for the regions of interest was 146 mm³ (range, 16.3–630 mm³) for tumors and 12.7 mm³ (range, 2.7–31 mm³) for muscle. Data are expressed as mean percent injected dose (ID) per gram. Tumor-to-muscle ratio was calculated as the ratio of mean percent ID per gram of tumor to that of muscle. The visual pattern of tumor FES uptake was also recorded descriptively.

Tissue Histologic Analysis

Excised tumors were fixed in 10% formalin and paraffin embedded. ERα immunohistochemistry was performed by using the Discovery XT automated platform (Ventana Medical Systems; Tucson, Ariz). Deparaffinization was performed followed by heat-induced epitope retrieval with CC1 buffer (tris-based; pH, 8.5) for 60 minutes at 100°C. ERα antibody (1:100 clone SP1; ThermoFisher, Waltham, Mass) was applied for 28 minutes at 37°C. After rinsing, OmniMap antirabbit–horse radish peroxidase antibody (Ventana Medical Systems) was applied for 8 minutes, followed by rinsing. Chromo Map 3,3'-diaminobenzidine (Biocare Medical, Pacheco, Calif) detection was applied, followed by rinsing and application of hematoxylin (CT Hematoxylin; Biocare Medical). Routine staining with hematoxylin-eosin was also performed. Slides were scanned at a magnification of 40× by using a whole-slide bright field imaging system (Aperio Image Scope software; Leica Biosystems, Buffalo Grove, Ill).

Slides were analyzed by a pathologist with subspecialty training in breast pathology (A.M.M., with 4 years of experience). Percentage tumor necrosis

was determined on the hematoxylin and eosin slides. ERα immunohistochemistry staining intensity (0 = none; 1 = weak; 2 = moderate; 3 = strong) and subjective percentage of cells with positive nuclear staining were scored.

Statistical Analyses

The nonparametric Mann-Whitney (Wilcoxon rank sum) test was used to compare ERα functional activity (reporter gene assay and quantitative polymerase chain reaction data) for the ethanol vehicle control versus estrogen-treated samples. FES uptake was compared between tumor xenografts by using the Mann-Whitney (Wilcoxon rank sum) test. P values less than .05 were considered to indicate statistical significance. Statistical analyses were performed by using software (R 3.3.2, R Foundation for Statistical Computing, Vienna, Austria; and GraphPad Prism 6.05, GraphPad, La Jolla, Calif).

Sample size calculations indicated that by using six mice with bilateral tumors (12 tumors total) per group, a t test at a 5% one-sided significance level will have approximately 90% power to detect an effect size of 1.19 (Cohen d value defined as the difference between the two means divided by the pooled standard deviation). Xenograft tumors of 231 WT ER cells were initially imaged as part of a control experiment for technical confirmation of FES uptake and were also included with imaging of the MDA-MB-231 and 231 G521R ER xenografts, which accounts for their relatively larger sample size. A relatively smaller number of MCF-7 tumors were imaged by using FES PET/CT simply as a positive control to confirm correct FES radiosynthesis and were not used for statistical comparison with the WT and mutant ER tumor models that used MDA-MB-231 cells.

Results

ERα Localization and Expression in Engineered Cell Lines

We observed nuclear localization of ERα protein in 231 WT ER and mutated 231 G521R ER cells and in MCF-7 cells that
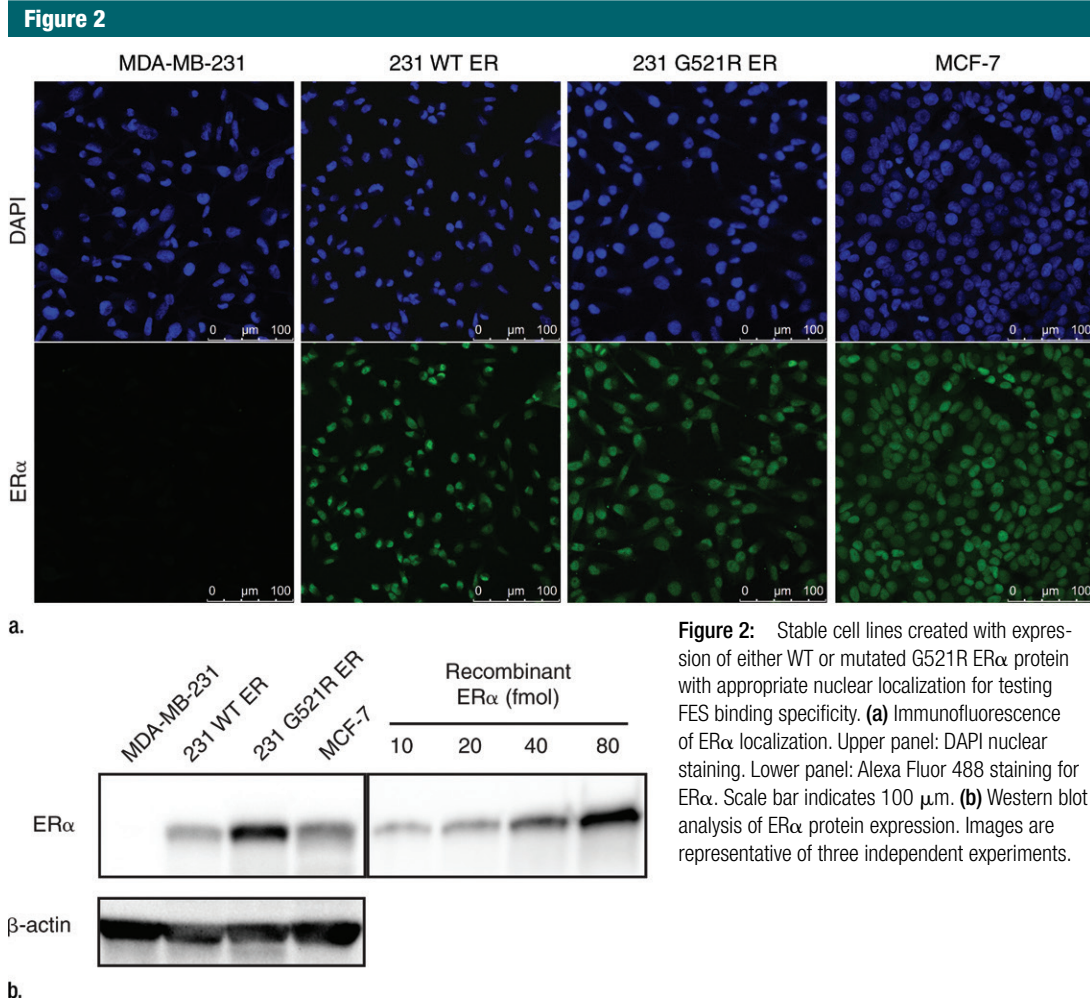
Figure 2

Figure 2: Stable cell lines created with expression of either WT or mutated G521R ERα protein with appropriate nuclear localization for testing FES binding specificity. **(a)** Immunofluorescence of ERα localization. Upper panel: DAPI nuclear staining. Lower panel: Alexa Fluor 488 staining for ERα. Scale bar indicates 100 μm. **(b)** Western blot analysis of ERα protein expression. Images are representative of three independent experiments.

express endogenous WT ERα (Fig 2a). No immunofluorescent staining was observed in the parental ER-negative MDA-MB-231 cells.

We then performed Western blot analysis to measure ERα protein levels in each of the cell lines. ERα expression was 0.2 fmol/mg total protein ± 0.2 (standard deviation) in MDA-MB-231 cells, 470 fmol/mg total protein ± 140 in 231 WT ER cells, 1478 fmol/mg total protein ± 214 in 231 G521R ER cells, and 811 fmol/mg total protein ± 180 in MCF-7 cells (Fig 2b).

ERα Functionally Inactive in 231 G521R ER Cells

Strong induction of ERα transcriptional activity was measured in the 231 WT ER cells after E_2 treatment (luciferase/β-galactoside activity, ethanol vs E_2: 0.19 ± 0.069 vs 3.6 ± 1.6, respectively; P = .03; Fig 3a). However, no significant estrogen-inducible transcriptional activity was measured in 231 G521R ER cells (ethanol vs E_2, 0.36 ± 0.028 vs 0.34 ± 0.0046, respectively; P = .70), similar to the parental ER-negative MDA-MB-231 cells (ethanol vs E_2, 0.11 ± 0.025 vs 0.10 ± 0.025, respectively; P = .66).

There was an eightfold induction of progesterone receptor messenger RNA (mRNA) expression in estrogen-treated 231 WT ER cells (relative fold change, ethanol vs E_2: 1.0 ± 0.06 vs 8.6 ± 0.51, respectively; P < .0001; Fig 3b). This was comparable

to progesterone receptor mRNA expression in MCF-7 cells after estrogen treatment (ethanol vs E_2, 1.0 ± 0.03 vs 7.2 ± 0.58, respectively; P < .0001). Similar to our results with the estrogen response element reporter gene assay, no induction of progesterone receptor mRNA was observed in 231 G521R ER (ethanol vs E_2, 1.0 ± 0.06 vs 1.2 ± 0.16, respectively; P = .50) and parental MDA-MB-231 cells (ethanol vs E_2, 1.0 ± 0.07 vs 1.0 ± 0.09, respectively; P = .84) treated with estrogen.

Loss of FES Uptake in 231 G521R ER Cells

By using a competitive binding assay, we observed FES binding competition curves in the 231 WT ER

cells (half-maximal inhibitory concentration, 0.10 nmol/L; 95% confidence interval: 0.09, 0.11) similar to that of ER-positive MCF-7 cells

(half-maximal inhibitory concentration, 0.13 nmol/L; 95% confidence interval: 0.12, 0.15) (Figure 4). However, there was no specific FES

binding in the 231 G521R ER cells, which behaved similarly to the parental MDA-MB-231 cells.

Loss of FES Uptake in 231 G521R ER Tumor Xenografts

Mean tumor volumes at the time of imaging for the MDA-MB-231, 231 WT ER, and 231 G521R ER xenografts were 174 mm³ ± 48, 135 mm³ ± 34, and 129 mm³ ± 34, respectively. FES uptake was observed in the 231 WT ER xenografts and was significantly greater than in the MDA-MB-231 xenografts (mean percent ID per gram, 0.85 ± 0.045 vs 0.42 ± 0.051, respectively; $P < .001$) and in muscle (mean percent ID per gram, 0.85 ± 0.045 vs 0.41 ± 0.0095, respectively; $P < .001$) (Fig 5). There was no significant FES uptake in the 231 G521R ER xenografts, which were similar to the negative control MDA-MB-231 xenografts (mean percent ID per gram, 0.49 ± 0.042 vs 0.42 ± 0.051, respectively; $P = .20$) and nonspecific muscle uptake (mean percent ID per gram, 0.49 ± 0.042 vs 0.41 ± 0.0095, respectively; $P = .06$). Tumor-to-muscle ratios in MDA-MB-231, 231 WT ER, and 231 G521R ER xenografts were 0.97 ± 0.07, 2.1 ± 0.10, and 1.1 ± 0.08, respectively (Fig 5). Strong FES uptake was observed in the positive control MCF-7 xenografts (tumor-to-muscle ratio, 7.2 ± 0.60). Visual assessment of the pattern of tumor FES uptake demonstrated homogeneous central uptake in MCF-7 xenografts and heterogeneous peripheral uptake in the 231 WT ER xenografts (Fig 5a).

ERα protein expression in the excised tumors was determined by using immunohistochemistry and Western blot analysis (Fig 5a; Table). Strong, relatively homogeneous receptor expression was observed in the 231 G521R ER and MCF-7 xenografts. However, we observed central tumor necrosis ($40\% \pm 19$) on hematoxylin-eosin–stained slides and a heterogeneous ERα immunostaining pattern in the 231 WT ER xenografts, which corresponds to the heterogeneous peripheral FES uptake pattern observed by using PET.

Figure 3
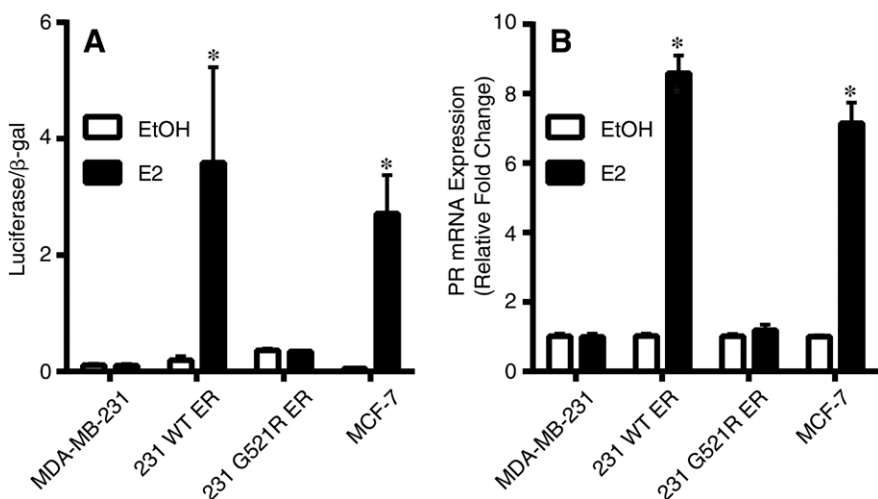
Figure 3: Bar graphs show ERα is functionally inactive in 231 G521R ER cells. *A,* Estrogen-deprived cells were transfected with estrogen response element–luciferase and β-galactosidase plasmids and then treated with ethanol *(EtOH)* vehicle or 10 nmol/L of 17β-estradiol *(E₂)* for 24 hours. Luciferase activity was measured and normalized to β-galactosidase activity. *B,* Progesterone receptor *(PR)* messenger RNA *(mRNA)* expression of estrogen-deprived cells was measured after 24 hours of treatment with ethanol or 10 nmol/L of E₂. Values represent the mean ± standard error of the mean of three independent experiments. ∗ $P <$ .05 compared with the corresponding ethanol control.

Figure 4
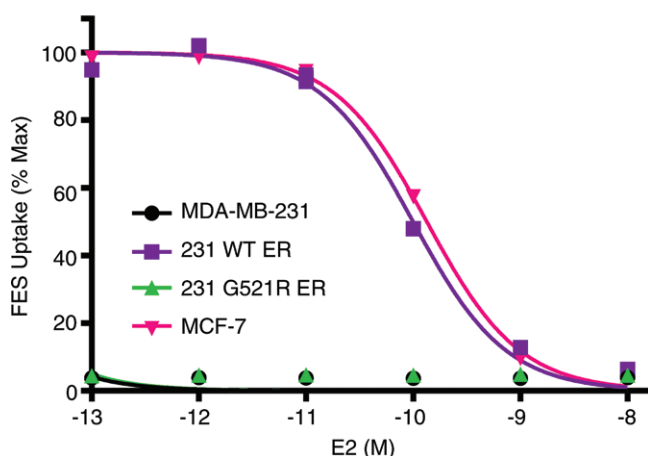
Figure 4: Graph shows loss of FES uptake in 231 G521R ER cells. Estrogen-deprived cells were treated with various concentrations of 17β-estradiol (E₂ range, 10^{-8} to 10^{-13} mol/L [*M*]) before addition of 0.037 MBq (1 μCi) FES for 1 hour. Decay-corrected counts per minute were normalized to wells containing FES with no cold E₂ for percent maximum uptake values. MDA-MB-231 and 231 G521R ER cell values were expressed relative to MCF-7. Values represent the mean ± standard error of the mean of three independent experiments.
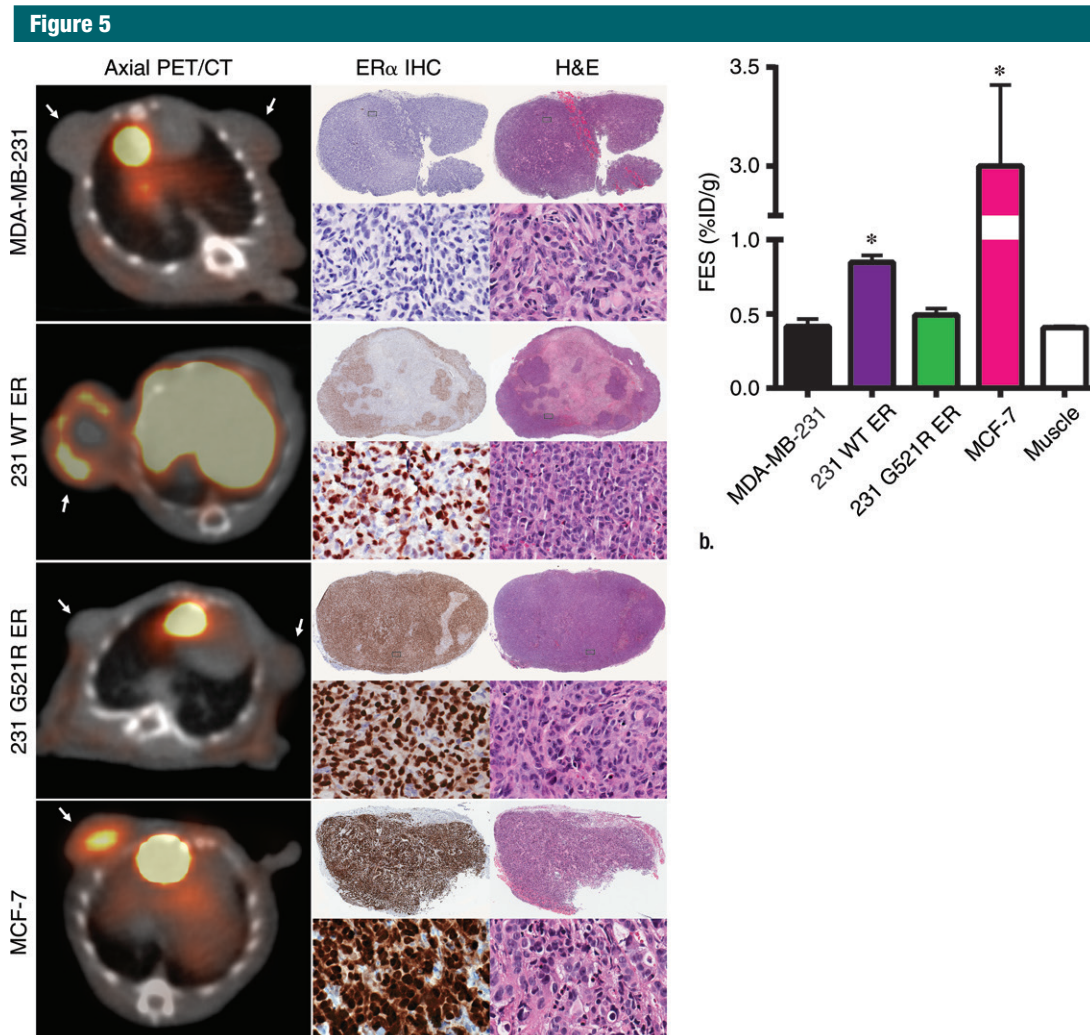
Figure 5

Figure 5: Loss of FES uptake in 231 G521R ER tumor xenografts. **(a)** Representative axial FES PET/CT images of tumor xenografts (arrows) grown in athymic nude female mice. Mice were injected with 9.25 MBq (250 μCi) of FES and images were obtained 1 hour after injection. FES uptake is also noted in gall bladder and liver because of physiologic hepatobiliary clearance. There are corresponding low- and high-power magnification images of ERα immunohistochemistry *(IHC)* and hematoxylin-eosin *(H&E)* staining of excised tumors (middle and left column in **a**, respectively). **(b)** Bar graph shows quantitative FES uptake assessed by mean percent ID per gram. Values are mean ± standard error of the mean. ∗ $P < .05$ compared tumor uptake in MDA-MB-231 and 231 G521R xenografts and compared with nonspecific muscle uptake. Included were eight MDA-MB-231 xenografts, 17 231 WT ER xenografts, and nine 231 G521R ER xenografts.

Discussion

We directly tested FES binding specificity by modification of a single amino acid in the ligand-binding domain of ERα that abolishes estradiol binding but preserves the remaining function of the receptor and by expressing this modified receptor in stable cell lines with comparative genetic background and phenotypes. These results support the hypothesis that there is no substantial FES binding to sites outside the ligand-binding pocket of ERα or to nonspecific cellular proteins.

High-fidelity binding of FES to the ligand-binding domain of ERα is important to prevent false-positive image interpretation because the presence of nonspecific radiotracer uptake may overestimate receptor expression and falsely indicate a high likelihood of response to endocrine therapy or insufficient antagonist drug dosing. By using genetically modified cell lines with in vitro binding assays and in vivo small-animal PET imaging, we demonstrated that FES binds to ERα with high specificity and is strictly dependent on an intact receptor ligand-binding pocket. FES uptake reflects receptor ligand-binding functionality rather than the amount of receptor protein expression. These results are a direct confirmation

Western, Immunohistochemistry, and Hematoxylin-Eosin Staining of Tumor Xenografts

Xenograft	ERα Protein Expression (fmol/mg)	Cells with ERα-Positive Nuclear Staining (%)	Tumor Necrosis (%)
MDA-MB-231	7.6 ± 9.0 (8)	0 ± 0* (8)	0.4 ± 0.5 (8)
231 WT ER	240 ± 80.3 (8)	72 ± 10† (13)	40 ± 19 (13)
231 G521R ER	461 ± 48.5 (8)	92 ± 7.6† (8)	12 ± 6.6 (8)
MCF-7	1680 ± 840 (4)	87 ± 15† (4)	28 ± 25 (4)

Note.—Data are mean ± standard deviation; data in percentages are number of tumors. Each tumor xenograft was the unit of observation and the level of analysis.

* Intensity scores were 0/3 for all samples.

† Intensity scores were 3/3 for all samples.

of FES binding specificity and expand the existing literature in the field.

Previously published work (7–10) provides indirect evidence of FES binding specificity. These include reports that show positive correlation ($r = 0.56–0.96$) between the amount of ERα protein in breast cancer lesions by using hydrogen 3–estradiol ligand-binding assays and immunohistochemistry and FES maximum standard uptake value. Likewise, preclinical work (17) that used ER-positive mouse mammary carcinoma cell lines demonstrated a 50% decrease in FES uptake at PET imaging in corresponding stable cells lines when ERα protein levels were decreased by 75% because of RNA interference. Similarly, a reduction in FES uptake paralleled the pharmacologic downregulation of ERα protein in ER-positive MCF-7 human breast cancer cells treated with fulvestrant for 24 hours (22). FES uptake was reduced by 86% and ERα protein levels were reduced by 60% at the highest dose of fulvestrant tested.

FES binding specificity was also shown by preclinical studies (5,15–18) that demonstrated decreases in uptake measured by tissue biodistribution or at PET imaging when unlabeled estradiol was co-injected. However, whereas estradiol competes with FES for binding ERα, once bound it induces proteasome-mediated degradation of ERα that results in an approximately 40% decrease in ERα protein within 1 hour (27). This occurs during the same time as FES incubation times, which could also result

in decreased FES uptake and is an inherent confounding factor to consider when interpreting these studies.

FES binding specificity can also be inferred from blockade observed with ERα antagonists (fulvestrant and tamoxifen) that also compete similarly to estradiol with FES for the ligand-binding domain (19–22). However, in many cases there is incomplete FES blockade, which was shown by 44% (seven of 16 patients) in a retrospective study (20) and 38% (six of 16 patients) in a subsequent prospective study (21). Incomplete FES blockade is likely secondary to inadequate antagonist drug dosing; however, the presence of nonspecific FES binding cannot be excluded.

Gain-of-function ESR1 mutations were identified in up to 40% of patients with metastatic, endocrine-resistant, ER-positive breast cancer and are associated with reduced survival (28,29). These mutations cluster in the ligand-binding domain, but unlike the inactivating G521R mutation, result in constitutively active ERα function. The effect of these activating mutations on FES uptake is unknown. It is possible that these receptors have reduced FES binding despite strong protein expression by immunohistochemistry, indicating that an ERα antagonist–based therapy may be less effective.

A potential limitation of our study is that the magnitude of FES uptake in the 231 WT ER tumor xenografts is relatively small (tumor-to-muscle ratio, 2.1 ± 0.10) compared with other

preclinical models (30,31). This could be because of endogenous circulating estrogen; however, this has not been shown to interfere with FES uptake in patients (32). Also, the relatively low amount of FES uptake in vivo may be partially explained by the amount of tumor necrosis that was highest in the 231 WT ER xenografts. Despite this challenge, significant differences in FES uptake could be observed between the WT and G521R mutant xenografts to confidently demonstrate binding specificity. Finally, our study does not address factors beyond FES uptake that may predict clinical benefit from endocrine therapy such as progesterone receptor (33).

To conclude, our results indicate that FES uptake reflects the receptor-ligand binding functionality rather than the amount of receptor protein expression. These results support the utility of FES PET imaging for assessment of intrapatient, intermetastatic tumor heterogeneity by localizing immunohistochemically ER-positive lesions lacking receptor binding functionality, which could direct further tissue biopsy for genomic analysis and optimize treatment.

References

1. Linden HM, Stekhova SA, Link JM, et al. Quantitative fluoroestradiol positron emission tomography imaging predicts response

to endocrine treatment in breast cancer. J Clin Oncol 2006;24(18):2793–2799.

2. Mortimer JE, Dehdashti F, Siegel BA, Trinkaus K, Katzenellenbogen JA, Welch MJ. Metabolic flare: indicator of hormone responsiveness in advanced breast cancer. J Clin Oncol 2001;19(11):2797–2803.

3. Venema CM, Apollonio G, Hospers GA, et al. Recommendations and technical aspects of 16α-[18F]fluoro-17β-estradiol PET to image the estrogen receptor in vivo: the Groningen experience. Clin Nucl Med 2016;41(11):844–851.

4. van Kruchten M, Glaudemans AW, de Vries EF, et al. PET imaging of estrogen receptors as a diagnostic tool for breast cancer patients presenting with a clinical dilemma. J Nucl Med 2012;53(2):182–190.

5. Kiesewetter DO, Kilbourn MR, Landvatter SW, Heiman DF, Katzenellenbogen JA, Welch MJ. Preparation of four fluorine-18-labeled estrogens and their selective uptakes in target tissues of immature rats. J Nucl Med 1984;25(11):1212–1221.

6. Yoo J, Dence CS, Sharp TL, Katzenellenbogen JA, Welch MJ. Synthesis of an estrogen receptor beta-selective radioligand: 5-[18F]fluoro-(2R,3S)-2,3-bis(4-hydroxyphenyl)pentanenitrile and comparison of in vivo distribution with 16alpha-[18F]fluoro-17beta-estradiol. J Med Chem 2005;48(20):6366–6378.

7. Mintun MA, Welch MJ, Siegel BA, et al. Breast cancer: PET imaging of estrogen receptors. Radiology 1988;169(1):45–48.

8. Peterson LM, Mankoff DA, Lawton T, et al. Quantitative imaging of estrogen receptor expression in breast cancer with PET and 18F-fluoroestradiol. J Nucl Med 2008;49(3):367–374.

9. Gemignani ML, Patil S, Seshan VE, et al. Feasibility and predictability of perioperative PET and estrogen receptor ligand in patients with invasive breast cancer. J Nucl Med 2013;54(10):1697–1702.

10. Chae SY, Kim SB, Ahn SH, et al. A randomized feasibility study of (18)F-fluoroestradiol PET to predict pathologic response to neoadjuvant therapy in estrogen receptor-rich postmenopausal breast cancer. J Nucl Med 2017;58(4):563–568.

11. van Kruchten M, de Vries EG, Brown M, et al. PET imaging of oestrogen receptors in patients with breast cancer. Lancet Oncol 2013;14(11):e465–e475.

12. Dehdashti F, Mortimer JE, Siegel BA, et al. Positron tomographic assessment of estrogen receptors in breast cancer: comparison with FDG-PET and in vitro receptor assays. J Nucl Med 1995;36(10):1766–1774.

13. Mortimer JE, Dehdashti F, Siegel BA, Katzenellenbogen JA, Fracasso P, Welch MJ. Positron emission tomography with 2-[18F]Fluoro-2-deoxy-D-glucose and 16alpha-[18F]fluoro-17beta-estradiol in breast cancer: correlation with estrogen receptor status and response to systemic therapy. Clin Cancer Res 1996;2(6):933–939.

14. Evangelista L, Guarneri V, Conte PF. 18F-fluoroestradiol positron emission tomography in breast cancer patients: systematic review of the literature & meta-analysis. Curr Radiopharm 2016;9(3):244–257.

15. Katzenellenbogen JA, Mathias CJ, VanBrocklin HF, Brodack JW, Welch MJ. Titration of the in vivo uptake of 16 alpha-[18F]fluoroestradiol by target tissues in the rat: competition by tamoxifen, and implications for quantitating estrogen receptors in vivo and the use of animal models in receptor-binding radiopharmaceutical development. Nucl Med Biol 1993;20(6):735–745.

16. Aliaga A, Rousseau JA, Ouellette R, et al. Breast cancer models to study the expression of estrogen receptors with small animal PET imaging. Nucl Med Biol 2004;31(6):761–770.

17. Paquette M, Tremblay S, Bénard F, Lecomte R. Quantitative hormone therapy follow-up in an ER+/ERαKD mouse tumor model using FDG and [11C]-methionine PET imaging. EJNMMI Res 2012;2(1):61.

18. Bénard F, Ahmed N, Beauregard JM, et al. [18F]Fluorinated estradiol derivatives for oestrogen receptor imaging: impact of substituents, formulation and specific activity on the biodistribution in breast tumour-bearing mice. Eur J Nucl Med Mol Imaging 2008;35(8):1473–1479.

19. McGuire AH, Dehdashti F, Siegel BA, et al. Positron tomographic assessment of 16 alpha-[18F] fluoro-17 beta-estradiol uptake in metastatic breast carcinoma. J Nucl Med 1991;32(8):1526–1531.

20. Linden HM, Kurland BF, Peterson LM, et al. Fluoroestradiol positron emission tomography reveals differences in pharmacodynamics of aromatase inhibitors, tamoxifen, and fulvestrant in patients with metastatic breast cancer. Clin Cancer Res 2011;17(14):4799–4805.

21. van Kruchten M, de Vries EG, Glaudemans AW, et al. Measuring residual estrogen receptor availability during fulvestrant therapy in patients with metastatic breast cancer. Cancer Discov 2015;5(1):72–81.

22. Heidari P, Deng F, Esfahani SA, et al. Pharmacodynamic imaging guides dosing of a selective estrogen receptor degrader. Clin Cancer Res 2015;21(6):1340–1347.

23. Fawell SE, Lees JA, White R, Parker MG. Characterization and colocalization of steroid binding and dimerization activities in the mouse estrogen receptor. Cell 1990;60(6):953–962.

24. Preisler-Mashek MT, Solodin N, Stark BL, Tyriver MK, Alarid ET. Ligand-specific regulation of proteasome-mediated proteolysis of estrogen receptor-alpha. Am J Physiol Endocrinol Metab 2002;282(4):E891–E898.

25. Fowler AM, Solodin NM, Valley CC, Alarid ET. Altered target gene regulation controlled by estrogen receptor-alpha concentration. Mol Endocrinol 2006;20(2):291–301.

26. Zhou D, Lin M, Yasui N, et al. Optimization of the preparation of fluorine-18-labeled steroid receptor ligands 16alpha-[18F]fluoroestradiol (FES), [18F]fluoro furanyl norprogesterone (FFNP), and 16beta-[18F]fluoro-5alpha-dihydrotestosterone (FDHT) as radiopharmaceuticals. J Labelled Comp Radiopharm 2014;57(5):371–377.

27. Alarid ET, Bakopoulos N, Solodin N. Proteasome-mediated proteolysis of estrogen receptor: a novel component in autologous down-regulation. Mol Endocrinol 1999;13(9):1522–1534.

28. Fribbens C, O'Leary B, Kilburn L, et al. Plasma ESR1 mutations and the treatment of estrogen receptor-positive advanced breast cancer. J Clin Oncol 2016;34(25):2961–2968.

29. Jeselsohn R, Buchwalter G, De Angelis C, Brown M, Schiff R. ESR1 mutations—a mechanism for acquired endocrine resistance in breast cancer. Nat Rev Clin Oncol 2015;12(10):573–583.

30. Fowler AM, Chan SR, Sharp TL, et al. Small-animal PET of steroid hormone receptors predicts tumor response to endocrine therapy using a preclinical model of breast cancer. J Nucl Med 2012;53(7):1119–1126.

31. Chan SR, Fowler AM, Allen JA, et al. Longitudinal noninvasive imaging of progesterone receptor as a predictive biomarker of tumor responsiveness to estrogen deprivation therapy. Clin Cancer Res 2015;21(5):1063–1070.

32. Peterson LM, Kurland BF, Link JM, et al. Factors influencing the uptake of 18F-fluoroestradiol in patients with estrogen receptor positive breast cancer. Nucl Med Biol 2011;38(7):969–978.

33. Mohammed H, Russell IA, Stark R, et al. Corrigendum: Progesterone receptor modulates ERα action in breast cancer. Nature 2015;526(7571):144.